Published November 25, 2015, doi:10.4049/jimmunol.1501140

Priming of Qualitatively Superior Human Effector CD8$^+$ T Cells Using TLR8 Ligand Combined with FLT3 Ligand

Anna Lissina*,†,1 Olivia Briceño,*,†,1 Georgia Afonso,‡,§,¶ Martin Larsen,*,† Emma Gostick,‖ David A. Price,‖ Roberto Mallone,‡,§,¶,# and Victor Appay*,†

The quality of Ag-specific CD8$^+$ T cell responses is central to immune efficacy in infectious and malignant settings. Inducing effector CD8$^+$ T cells with potent functional properties is therefore a priority in the field of immunotherapy. However, the optimal assessment of new treatment strategies in humans is limited by currently available testing platforms. In this study, we introduce an original model of in vitro CD8$^+$ T cell priming, based on an accelerated dendritic cell coculture system, which uses unfractionated human PBMCs as the starting material. This approach enables the rapid evaluation of adjuvant effects on the functional properties of human CD8$^+$ T cells primed from Ag-specific naive precursors. We demonstrate that a selective TLR8 agonist, in combination with FLT3L, primes high-quality CD8$^+$ T cell responses. TLR8L/FLT3L-primed CD8$^+$ T cells displayed enhanced cytotoxic activity, polyfunctionality, and Ag sensitivity. The acquisition of this superior functional profile was associated with increased T-bet expression induced via an IL-12–dependent mechanism. Collectively, these data validate an expedited route to vaccine delivery or optimal T cell expansion for adoptive cell transfer. ***The Journal of Immunology*****, 2016, 196: 000–000.**

Cytotoxic activity, polyfunctionality, and Ag sensitivity predict CD8$^+$ T cell efficacy against infected or dysregulated cells (1, 2). Potent cytotoxic activity is necessary for the elimination of diseased cells, and demonstrations of synergy between IFN-γ and TNF during the induction of permanent growth arrest in cancerous or infected cells have highlighted the importance of T cell polyfunctionality (i.e., the capacity to produce multiple effector cytokines simultaneously) (3). In addition, high levels of Ag sensitivity endow T cells with the capacity to recognize cognate peptide–MHC class I (pMHCI) complexes at low densities on the target cell surface, and thus to act swiftly against infected cells or to break the immune tolerance associated with cancer (4). However, the induction of de novo CD8$^+$ T cell responses with such protective attributes in humans has proven difficult in the settings of vaccination and adoptive cell therapy (5, 6). Dendritic cells (DCs) govern the nature of CD8$^+$ T cell responses primed from naive precursors, via the provision of processed Ags in the form of pMHCI molecules, together with other important signals, including costimulatory interactions and inflammatory cytokines. Much effort has therefore been devoted to the modulation of DC function for the optimization of CD8$^+$ T cell immunity (7). Adjuvants, such as TLR ligands, can further improve the immunogenicity of soluble protein and peptide Ags by mimicking pathogen-associated "danger" signals (8, 9). Combinatorial assessments of various modalities are therefore required to enhance the efficacy of immunotherapeutic interventions.

However, it is difficult to study the effects of potential adjuvants on human CD8$^+$ T cell responses due to the lack of a suitable model. Although the widespread use of murine systems has greatly advanced our knowledge of TLR function and DC/T cell interactions, there are significant biological differences between mice and humans that complicate simple extrapolation between species. For instance, the cellular distribution of TLR8 is entirely different between humans and mice and is considered to be nonfunctional in the latter (10). As a consequence, the adjuvant properties of TLR8-selective agonists have not been fully assessed (11, 12). Moreover, traditional in vitro priming protocols that use human material rely on populations of inflammatory monocyte-derived DCs (moDCs) generated in a two-stage process from PBMC-purified CD14$^+$ monocytes (13). In this setting, differentiation is achieved using a combination of GM-CSF and IL-4 prior to maturation with a mixture of inflammatory cytokines or LPS (14, 15). Although adequate for many purposes, this strategy has a number of limitations. In particular, the initial preparation of moDCs is laborious and time consuming. More importantly, it is limited to one subset of APCs, and no attempt is made to evaluate the role of conventional DCs and other resident blood cells (e.g., CD4$^+$ T cells and NK cells) in the priming process.

To circumvent these drawbacks, we developed an innovative model of human CD8$^+$ T cell priming. This original in vitro approach is based on the rapid mobilization of DCs directly from unfractionated PBMCs, adapted from an earlier method designed to detect low-frequency memory T cell responses (15). Importantly, this strategy enables side-by-side studies of multiple test

*Sorbonne Universités, Université Pierre et Marie Curie Univ Paris 06, DHU FAST, Centre d'Immunologie et des Maladies Infectieuses, 75013 Paris, France; †INSERM U1135, Centre d'Immunologie et des Maladies Infectieuses, Hôpital Pitié-Salpêtrière, 75013 Paris, France; ‡INSERM U1016, Institut Cochin, 75014 Paris, France; §CNRS, UMR8104, Institut Cochin, 75014 Paris, France; ¶Université Paris Descartes, Sorbonne Paris Cité, Faculté de Médecine, 75006 Paris, France; ‖Institute of Infection and Immunity, Cardiff University School of Medicine, Cardiff CF14 4XN, United Kingdom; and #Assistance Publique-Hôpitaux de Paris, Hôpital Cochin, Service de Diabétologie, 75014 Paris, France

[1]A.L. and O.B. participated equally in the work.

ORCID: 0000-0003-1375-4816 (M.L.).

Received for publication May 15, 2015. Accepted for publication October 8, 2015.

This work was supported by the French Agence Nationale de la Recherche (Projects ANR-09-JCJC-0114-01 and ANR-14-CE14-0030-01), the Fondation Recherche Médicale (Project DEQ20120323690), and INSERM-Transfert. D.A.P. is a Wellcome Trust Senior Investigator, and R.M. is an INSERM Avenir and Assistance Publique-Hôpitaux de Paris-INSERM Contrat Hospitalier de Recherche Translationelle Investigator.

Address correspondence and reprint requests to Dr. Victor Appay, INSERM U1135, Centre d'Immunologie et des Maladies Infectieuses, Hôpital Pitié-Salpêtrière, 91 Boulevard de l'Hôpital, 75013 Paris, France. E-mail address: victor.appay@upmc.fr

The online version of this article contains supplemental material.

Abbreviations used in this article: B-LCL, B-lymphoblastoid cell line; DC, dendritic cell; mDC, myeloid DC; PBSE, Pacific Blue succinimidyl ester; pDC, plasmacytoid DC; pMHCI, peptide–MHC class I; TLR8L, TLR8 ligand.

Copyright © 2015 by The American Association of Immunologists, Inc. 0022-1767/15/$30.00

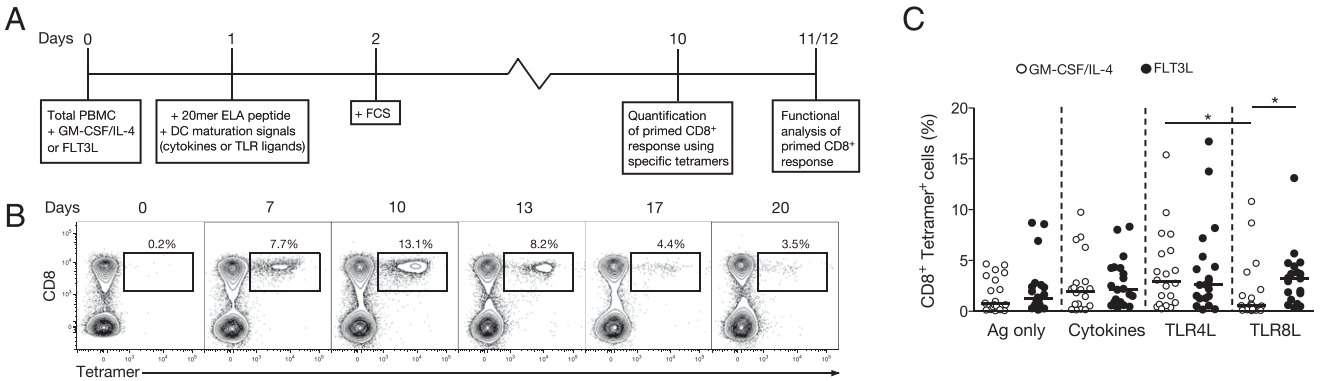

FIGURE 1. In vitro CD8$^+$ T cell priming and the magnitude of TLR8L-primed Ag-specific cells. (**A**) Outline of the in vitro CD8$^+$ T cell priming system using unfractionated PBMC samples. (**B**) Representative flow cytometry data showing the kinetics of ELA-specific CD8$^+$ T cell priming in the presence of GM-CSF/IL-4 and a mixture of inflammatory cytokines. Plots are gated on viable CD3$^+$ lymphocytes after aggregate exclusion. Numbers refer to percentages of ELA-HLA-A2 tetramer$^+$ cells within the total CD8$^+$ T cell population. (**C**) Response magnitudes for ELA-specific CD8$^+$ T cell populations primed under different conditions from several healthy HLA-A2$^+$ donor PBMC samples. Ag only (no maturation signal), cytokine mixture (TNF, IL-1β, PGE_2, and IL-7), TLR4L (LPS), or TLR8L (ssRNA40) were each used in combination with either GM-CSF/IL-4 or FLT3L supplementation. Horizontal bars indicate median values. Statistical comparisons between groups were performed using the Wilcoxon signed rank test: $*p < 0.05$.

parameters in a standardized system with quantitative and qualitative readouts of the primed Ag-specific CD8$^+$ T cell response. In this study, we used our new approach to compare conventional adjuvant combinations alongside the largely uncharacterized ssRNA40 TLR8 ligand (TLR8L).

Materials and Methods

Flow cytometry reagents

Standard and CD8-null ELA/HLA-A2 tetramers were produced as described previously (16, 17). The CD8-null ELA/HLA-A2 complex incorporates a compound D227K/T228A mutation in the α3 domain that abrogates CD8 binding without impacting on the TCR docking platform (18). Directly conjugated mAbs were purchased from commercial sources as follows: 1) anti–CD8-allophycocyanin-Cy7, anti–CD45RA-V450, anti–CCR7-PE-Cy7, anti–CD107a-PE-Cy5, anti–IFN-γ-AlexaFluor 700, anti–TNF-PE-Cy7, and anti–granzyme-B-V450 (BD Biosciences); 2) anti–CD3-ECD (Beckman Coulter); 3) anti–CD28-AlexaFluor 700 (BioLegend); 4) anti–T-bet-Alexa Fluor 647 (eBiosciences); 5) anti–MIP-1β-FITC (R&D Systems); 6) anti–IL-2-allophycocyanin (Miltenyi Biotec); and 7) anti–perforin-BD48-FITC (Abcam). The amine-reactive viability dye Aqua (Life Technologies) was used to eliminate dead cells from the analysis. Intracellular staining for T-bet was performed using the Transcription Factor Buffer Set (BD Pharmingen), according to the manufacturer's instructions. Intracellular staining for granzyme B and perforin-BD48 was compatible with this procedure. Staining with all other reagents was conducted according to standard protocols (19, 20). Data were acquired using an LSR Fortessa flow cytometer (BD Biosciences) and analyzed with FlowJo software version 9.3.7 (Tree Star).

Peptides

All peptides were synthesized commercially at >95% purity (Biosynthesis). The ELA-10 peptide (ELAGIGILTV; Melan-A/MART-1 residues $26–35_{A27L}$) was used to pulse target cells in functional assays. The ELA-20 peptide (YTAAEELAGIGILTVILGVL; Melan-A/MART-1 residues $21–40_{A27L}$) was used for in vitro priming. The ELA-20Ct peptide (GHGHSYTAAEELAGIGILTV; Melan-A/MART-1 residues $16–35_{A27L}$) was tested in early presentation and stability experiments (Supplemental Fig. 1).

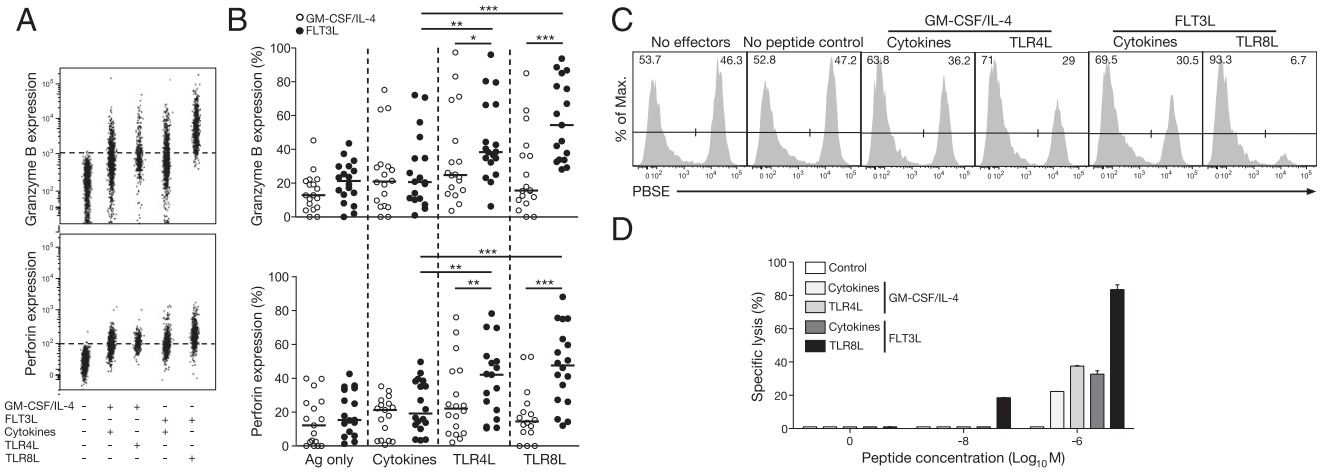

FIGURE 2. Greater cytotoxic potential of CD8$^+$ T cells primed in vitro with an FLT3L/TLR8L combination. (**A**) Representative flow cytometry plots showing granzyme B (*top panel*) or perforin (*bottom panel*) expression by ELA-specific CD8$^+$ T cells primed under different conditions. (**B**) Granzyme B (*top graph*) and perforin (*bottom graph*) expression by ELA-specific CD8$^+$ T cells primed under different conditions from several healthy HLA-A2$^+$ donor PBMC samples. Horizontal bars indicate median values. Statistical comparisons between groups were performed using the Wilcoxon signed rank test: $*p < 0.05$, $**p < 0.01$, $***p < 0.001$. (**C**) Representative flow cytometry data from a fluorometric cytotoxicity assay showing the disappearance of ELA peptide-pulsed PBSE$^+$ HLA-A2$^+$ B-LCL target cells relative to non–peptide-pulsed PBSE$^-$ HLA-A2$^+$ B-LCL control cells in the presence of ELA-specific CD8$^+$ T cells primed under different conditions. Numbers indicate the percentages of control (*upper left*) and target (*upper right*) B-LCL cells. (**D**) Specific lysis of HLA-A2$^+$ B-LCL target cells presenting the indicated concentrations of exogenously loaded ELA peptide in the presence of ELA-specific CD8$^+$ T cells primed under different conditions. A noncognate population of CD8$^+$ T cells derived from the same HLA-A2$^+$ donor and cultured under similar conditions to the ELA-specific CD8$^+$ T cell population was used as a control. Error bars represent SD from the mean of two replicates.

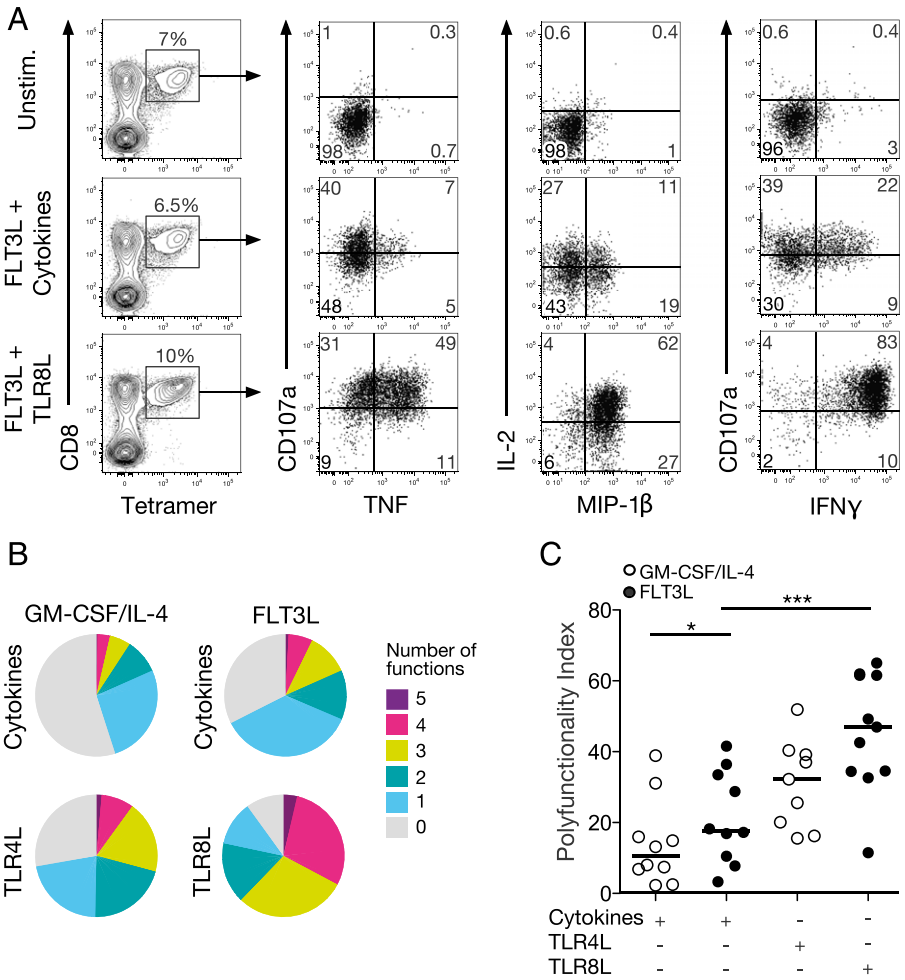

FIGURE 3. Polyfunctionality of FLT3L/TLR8L-primed CD8$^+$ T cells. (**A**) Representative flow cytometry plots showing cytokine production (IFN-γ, MIP-1β, TNF, and IL-2) and degranulation (CD107a) in response to Ag stimulation. ELA-specific CD8$^+$ T cells primed under the indicated conditions were incubated with media alone (*top row*) or ELA peptide-pulsed HLA-A2$^+$ B-LCL target cells (*middle* and *bottom rows*). Primed ELA-specific CD8$^+$ T cells were quantified as tetramer$^+$ cells within the total CD8$^+$ population (*left column*). Function plots are gated on viable CD3$^+$CD8$^+$ tetramer$^+$ lymphocytes (*middle* and *right columns*). Numbers in each quadrant refer to the percentages of primed ELA-specific CD8$^+$ T cells expressing the indicated combinations of functions. (**B**) Averaged pie chart representations of background-adjusted polyfunctional profiles for ELA-specific CD8$^+$ T cells primed under different conditions from 10 healthy donors. Pie segments and colors correspond to the proportions of ELA-specific CD8$^+$ T cells expressing the indicated number of functions, respectively. (**C**) Polyfunctionality indices for ELA-specific CD8$^+$ T cell populations, calculated from the data depicted in (B). Horizontal bars indicate median values. Statistical comparisons between groups were performed using the Wilcoxon signed rank test: $*p < 0.05$, $***p < 0.001$.

PBMCs and cell lines

PBMC samples were obtained from healthy HLA-A2$^+$ individuals via standard protocols and cryopreserved before use in CD8$^+$ T cell priming assays. The ELA-specific CD8$^+$ T cell line Mel9916 was generated by in vitro priming and purified by flow cytometric sorting of ELA/HLA-A2 tetramer$^+$ events. An HLA-A2$^+$ EBV–transformed B-lymphoblastoid cell line (B-LCL) was used to present the ELA-10 peptide in activation assays. The HLA-A2$^+$ tumor cell line Me275 was used to present the naturally processed Melan-A/MART-1 epitope (AAGIGILTV; Melan-A/MART-1 residues 27–35). The HLA-A2$^+$ Melan-A/MART-1$^-$ tumor cell line Me241 was used as a negative control.

In vitro priming of naive Melan-A/MART-1 Ag-specific CD8$^+$ T cells

Naive precursors specific for the HLA-A2–restricted Melan-A/MART-1 epitope ELA (ELAGIGILTV; Melan-A/MART-1 residues 26–35$_{A27L}$) were primed in vitro using an accelerated DC coculture protocol. Thawed PBMCs were resuspended in AIM medium (Invitrogen), supplemented with either GM-CSF (1000 IU/ml; Miltenyi Biotec) and IL-4 (500 IU/ml; InvivoGen) or FLT3L (50 ng/ml; R&D Systems), and plated out at 5×10^6 cells/well in a 24-well tissue culture plate (day 0). After 24 h (day 1), maturation of resident DCs was induced under one of the following conditions: 1) a standard mixture of inflammatory cytokines comprising TNF (1000 U/ml), IL-1β (10 ng/ml), IL-7 (0.5 ng/ml), and PGE_2 (1 μM; R&D Systems) (15); 2) LPS (0.1 μg/ml; Invivogen); or 3) ssRNA40 (0.5 μg/ml; InvivoGen). The ELA-20 peptide was added together with the DC maturation reagents at a final concentration of 1 μM. On day 2, FCS (Life Technologies) was added to 10% by volume per well. Fresh RPMI 1640 medium (Life Technologies) enriched with 10% FCS was used to replace the medium every 3 d. ELA-specific CD8$^+$ T cell frequency and phenotype were typically determined on day 10. Purified naive and memory CD8$^+$ T cell subsets (Supplemental Fig. 2) were obtained using the T cell Enrichment Column Kit (R&D Systems). An unconjugated anti–IL-12p70 blocking Ab (R&D Systems) was added at a final concentration of 10 μg/ml on days 0, 1, and 2 in later priming experiments (Fig. 6). An unconjugated mouse IgG1 isotype-matched Ab was used as a nonblocking control (anti–IL-12$^-$).

Polyfunctionality assay

ELA-primed PBMCs containing ~5×10^4 ELA/HLA-A2 tetramer$^+$ CD8$^+$ T cells were incubated with ELA-10 peptide–pulsed HLA-A2$^+$ B-LCL target cells at an E:T ratio of 1:10 in the presence of anti–CD107a for 6 h at 37°C. Monensin (2.5 μg/ml; Sigma-Aldrich) and brefeldin A (5 μg/ml; Sigma-Aldrich) were added for the final 5 h. Parallel assays were conducted with unpulsed HLA-A2$^+$ B-LCL target cells to evaluate nonspecific background activation. Intracellular cytokine staining was performed as described previously (21). Data were acquired using an LSR Fortessa flow cytometer (BD Biosciences) and analyzed with FlowJo software version 9.3.7 (Tree Star). Pie charts were constructed using SPICE software (National Institute of Allergy and Infectious Diseases), and polyfunctionality indices were calculated as described previously (22).

Fluorometric cytotoxicity assay

ELA-10 peptide-pulsed HLA-A2$^+$ B-LCL target cells were labeled with Pacific Blue succinimidyl ester (PBSE; 10 μM) to allow flow cytometric separation from unpulsed HLA-A2$^+$ B-LCL control cells, which were left unlabeled (PBSE$^-$). A total of 10^4 PBSE$^+$ target and 10^4 PBSE$^-$ control cells were incubated with CD8-enriched PBMCs containing 5×10^4 primed ELA-specific CD8$^+$ T cells for 12 h at 37°C. Control assays were set up in parallel either without effectors or with noncognate CD8$^+$ T cells at the same E:T ratio (5:1). After harvesting, cells were stained with Aqua, anti–CD3-ECD, anti–CD8-allophycocyanin-Cy7, and anti–CD19-FITC prior to acquisition using an LSR Fortessa flow cytometer (BD Biosciences). Lytic activity was calculated as a function of PBSE$^+$ target cell elimination relative to internal PBSE$^-$ control cells.

Statistical analysis

Comparisons between groups were performed using the Wilcoxon signed rank test in Prism 5 (GraphPad). A p value <0.05 was considered significant.

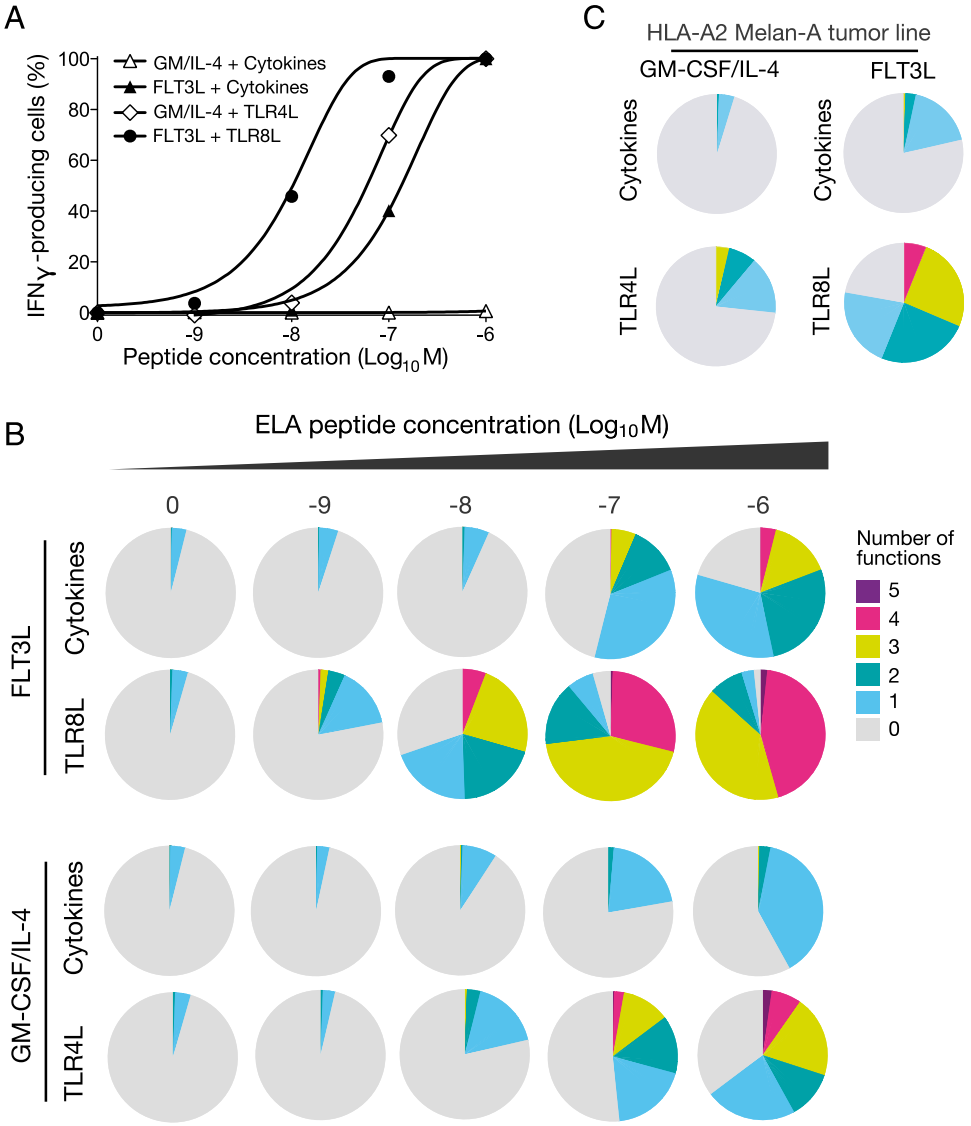

FIGURE 4. High Ag sensitivity of FLT3L/TLR8L-primed CD8$^+$ T cells. (**A**) Normalized IFN-γ production curves for ELA-specific CD8$^+$ T cells primed under different conditions. HLA-A2$^+$ B-LCL target cells were pulsed with ELA peptide across a range of concentrations and used to stimulate ELA-specific CD8$^+$ T cells in standard intracellular cytokine staining assays. Data are representative of two independent experiments. (**B**) Polyfunctional profiles of ELA-specific CD8$^+$ T cells primed under the indicated conditions. HLA-A2$^+$ B-LCL target cells were pulsed with ELA peptide across a range of concentrations and used to stimulate ELA-specific CD8$^+$ T cells prior to flow cytometric analysis. (**C**) Polyfunctional profiles of ELA-specific CD8$^+$ T cells responding to natural levels of the Melan-A/MART-1 Ag presented by an HLA-A2$^+$ melanoma cell line. An HLA-A2$^+$ Melan-A/MART-1$^-$ tumor cell line was used as a negative control (data not shown). Data in (B) and (C) are depicted in pie chart representations averaged from two independent experiments conducted with HLA-A2$^+$ PBMCs from two different donors with equivalent frequencies of expanded cells across all conditions.

Results

Design of an accelerated DC coculture system to prime T cells in vitro

The experimental outline of our new priming approach, starting from unfractionated PBMCs, is summarized in Fig. 1A. As circulating human DCs are rare, precursors (in particular CD14$^+$ monocytes) within the starting PBMC material were mobilized using GM-CSF/IL-4 and matured with a mixture of inflammatory cytokines including TNF, IL-1β, and PGE_2. IL-7 was also added to facilitate the priming of naive T cells upon Ag-driven activation, as described previously during the optimization of our accelerated DC coculture protocol (15, 23). Alternatively, DC mobilization was achieved by exposure of PBMCs to FLT3 ligand (FLT3L), which has demonstrable T cell priming efficacy in animal studies (24). GM-CSF/IL-4 and FLT3L have been shown to act on various immune cell subsets and mobilize distinct populations of DCs (25–27). To ensure that sufficient numbers of Ag-specific CD8$^+$ T cells were present in the naive pool for experimental purposes, we focused our analysis on the Melan-A/MART-1 epitope EAAGIGILTV$_{26–35}$, which is recognized at remarkably high precursor frequencies in HLA-A2$^+$ individuals (28, 29). The polyclonal composition of this naturally generated Melan-A/MART-1–specific repertoire presents distinct advantages over the TCR transgenic mouse models that are typically used to study Ag-driven adaptive immunity (30, 31). To ensure optimal immunogenicity, we used the heteroclitic sequence ELAGIGILTV (ELA) (32). Moreover, the ELA epitope was incorporated into a 20-mer synthetic long peptide (ELA-20) as a means of limiting Ag display to DCs with cross-presentation capacity (33–35). Prior to experimentation, we verified that the ELA-20 peptide required active processing. Specifically, we showed that ELA-20 was not presented directly by HLA-A2 (Supplemental Fig. 1A) and was not subjected to nonspecific cleavage by enzymes present in serum (Supplemental Fig. 1B).

Next, we evaluated the optimal parameters for ELA-specific CD8$^+$ T cell priming in our system. An ELA-20 concentration of 1 μM consistently generated sufficiently large populations of primed cells for functional characterization (data not shown) and was therefore chosen for all downstream assays. Primed ELA-specific CD8$^+$ T cells peaked on day 10 (Fig. 1B), following identical kinetics and achieving comparable magnitudes with both the GM-CSF/IL-4 and FLT3L protocols (Supplemental Fig. 2A). Subsequent experiments were therefore conducted over this time frame. We also confirmed that primed ELA-specific CD8$^+$ T cells originated from the naive (CCR7$^+$CD45RA$^+$) pool (Supplemental Fig. 2B, 2C). After priming, the vast majority of ELA/HLA-A2 tetramer$^+$CD8$^+$ T cells displayed phenotypic hallmarks of Ag-driven expansion, predominantly differentiating into the effector

memory (CCR7$^-$CD45RA$^-$) compartment (Supplemental Fig. 2D, 2E). No differences in terms of differentiation status were observed between ELA-specific CD8$^+$ T cell populations primed with either GM-CSF/IL-4 or FLT3L (Supplemental Fig. 2E).

Human CD8$^+$ T cell priming with a selective TLR8 agonist

In subsequent experiments, we used our validated system to study the effect of a recently available TLR8L (ssRNA40), compared in parallel with the standard mixture of inflammatory cytokines (TNF, IL-1β, PGE_2, and IL-7), or with LPS, an extensively studied TLR4L. Either TLR4L or TLR8L was introduced during the DC maturation step, in lieu of the inflammatory cytokine mixture. Tetramer-based enumeration of ELA-specific CD8$^+$ T cell populations expanded in parallel revealed no major differences in the magnitude of priming across the three maturation conditions tested (Fig. 1C). However, the GM-CSF/IL-4/TLR8L combination primed significantly fewer ELA-specific CD8$^+$ T cells compared with the FLT3L/TLR8L combination, highlighting differences in the way that GM-CSF/IL-4 and FLT3L modulate subsets of APCs. To support this point, we subjected purified CD14$^+$ monocytes to GM-CSF/IL-4 or FLT3L before introducing different maturation factors into the culture medium (Supplemental Fig. 3). As expected, GM-CSF/IL-4 but not FLT3L treatment resulted in the differentiation of monocytes into moDCs (with downregulation of CD14 from the surface of GM-CSF/IL-4–treated cells). However, although our cytokine mixture and TLR4L both induced the maturation of these cells (measured by upregulation of HLA-DR and CD86 on the surface of moDCs), TLR8L had no effect. The failure of GM-CSF/IL-4–induced moDCs to respond to TLR8L stimulation (despite expression of TLR8) provides one potential explanation for the poor T cell priming capacity of the GM-CSF/IL-4/TLR8L combination in our system. These findings highlight the limitations of moDCs and question the suitability of these in vitro–generated inflammatory cells for the study of potential adjuvants. Unfractionated PBMCs may therefore be a preferable alternative to isolated moDCs, the use of which would have overlooked the FLT3L/TLR8L effect on T cell priming. Notably, FLT3L/TLR8L-primed ELA-specific CD8$^+$ T cells possessed significantly greater cytotoxic potential, as assessed by the expression of granzyme B and perforin, compared with their counterparts primed under other conditions (Fig. 2A, 2B). This observation was confirmed in APC lysis assays, where CD8$^+$ T cells primed in the presence of FLT3L/TLR8L killed more than twice as many target cells loaded with 1 μM ELA-10 than CD8$^+$ T cells primed under any other condition (Fig. 2C, 2D). Moreover, only FLT3L/TLR8L-primed CD8$^+$ T cells were capable of eliminating targets presenting ELA-10 at a concentration of 10 nM.

Qualitatively superior human CD8$^+$ T cell responses primed with FLT3L/TLR8L

Next, we assessed the ability of primed CD8$^+$ T cells to deploy multiple effector functions in response to Ag encounter. In these assays, we measured the simultaneous induction of IFN-γ, MIP-1β, TNF, and IL-2 together with surface mobilization of CD107a (Fig. 3A). Although GM-CSF/IL-4 and FLT3L in conjunction with the cytokine mixture generated ELA-primed CD8$^+$ T cells expressing similar levels of cytotoxic molecules (Fig. 2A, 2B), FLT3L treatment elicited greater frequencies of polyfunctional cells compared with GM-CSF/IL-4 (Fig. 3B, *top row*). Moreover, ELA-specific CD8$^+$ T cells primed using the FLT3L/TLR8L combination displayed the highest levels of polyfunctionality (Fig. 3B). These differences were statistically significant in terms of the calculated polyfunctionality index across individual PBMC donors (Fig. 3C).

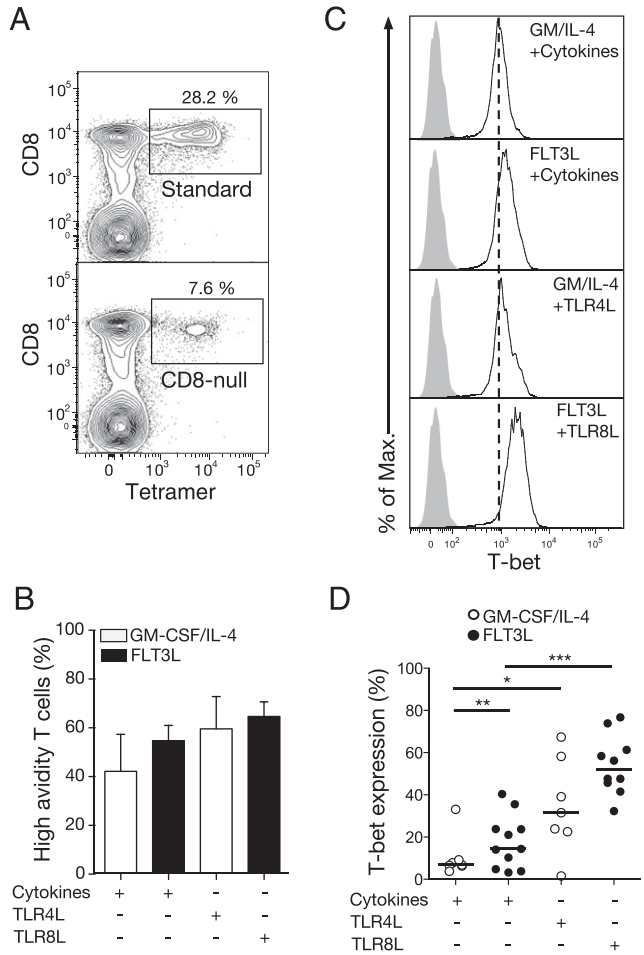

FIGURE 5. TCR avidity and T-bet expression in primed CD8$^+$ T cells. (**A**) Representative flow cytometry plots showing standard or CD8-null ELA/HLA-A2 tetramer staining of primed ELA-specific CD8$^+$ T cells. Plots are gated on viable CD3$^+$ lymphocytes after aggregate exclusion. Numbers refer to percentages of tetramer$^+$ cells within the total CD8$^+$ population. (**B**) Percentages of high-avidity ELA-specific CD8$^+$ T cells primed using either GM-CSF/IL-4 or FLT3L in combination with a mixture of inflammatory cytokines (TNF, IL-1β, PGE_2, and IL-7) or TLR ligands. These percentages were calculated from the corresponding CD8-null/standard ELA/HLA-A2 tetramer$^+$ cell ratios. Data are averaged over four independent experiments. Error bars represent SD from the mean. (**C**) Representative flow cytometry plots showing intracellular T-bet expression (white histograms) by ELA-specific CD8$^+$ T cells primed under different conditions. Gray histograms depict isotype control staining and vertical dotted lines indicate the mean fluorescence intensity (MFI) of T-bet staining for the weakest priming condition. (**D**) Intracellular T-bet expression by ELA-specific CD8$^+$ T cells primed under different conditions. Horizontal bars indicate median values. Statistical comparisons between groups were performed using the Wilcoxon signed rank test: $^*p < 0.05$, $^{**}p < 0.01$, $^{***}p < 0.001$.

Ag sensitivity, a major determinant of CD8$^+$ T cell functionality, was evaluated via cognate peptide titration in IFN-γ secretion assays. FLT3L/TLR8L-primed ELA-specific CD8$^+$ T cells displayed the highest Ag sensitivity, with a typical EC_{50} value (7.45×10^{-9} M) ~1 or 2 orders of magnitude lower compared with the GM-CSF/IL-4/TLR4L (5.77×10^{-8} M) or FLT3L/cytokine (1.36×10^{-7} M) combinations, respectively (Fig. 4A). IFN-γ production by GM-CSF/IL-4/cytokine–primed ELA-specific CD8$^+$ T cells was negligible. These differences in Ag sensitivity between conditions extended across the full spectrum of effector functions, enabling FLT3L/TLR8L-primed CD8$^+$ T cells to deploy multiple effector functions at ELA-10 peptide concentrations as low as 1 nM (Fig. 4B),

equivalent to the amount of Ag presented in physiological settings. Crucially, FLT3L/TLR8L-primed ELA-specific CD8$^+$ T cells were indeed capable of mounting polyfunctional responses to an HLA-A2$^+$ melanoma cell line naturally expressing the endogenous Melan-A/MART-1 Ag (Fig. 4C). In contrast, the same tumor cell line was not recognized efficiently by ELA-specific CD8$^+$ T cells primed under other test conditions (Fig. 4C).

Mechanistic insights into TLR8L-mediated adjuvant effects

Next, we explored the mechanisms involved in the acquisition of superior functional attributes by FLT3/TLR8L-primed CD8$^+$ T cells. It is established that TCR avidity, defined as the collective affinities of multiple monomeric TCR/pMHC interactions, can greatly influence Ag sensitivity and thereby dictate the functional profile of CD8$^+$ T cells in response to cognate Ag (21, 36). Accordingly, we used standard and CD8-null ELA/HLA-A2 tetramers in parallel to quantify this parameter across different priming conditions (Fig. 5A). CD8-null tetramers enable the selective detection of high-avidity Ag-specific CD8$^+$ T cells (17). Despite a small increase within the FLT3/TLR8L-primed CD8$^+$ T cell population, no statistically significant differences in TCR avidity were detected across any of the test conditions (Fig. 5B).

The expression of effector molecules such as granzyme B, perforin, and IFN-γ is tightly controlled in CD8$^+$ T cells by the T-box transcription factor T-bet (also known as Tbx-21) (37). We therefore assessed the intracellular expression of T-bet in CD8$^+$ T cells upon priming. Significantly higher T-bet expression levels were detected in ELA-specific CD8$^+$ T cells primed with FLT3L/TLR8L compared with other combinations (Fig. 5C, 5D). T-bet expression is regulated by IL-12 (38), which is known to be secreted by myeloid DCs upon TLR8 ligation (11). To assess the relationship between IL-12 levels and T-bet induction in our in vitro priming system, an anti–IL-12p70 blocking Ab was administered daily during the first 3 d of culture. This intervention led to a significant drop in T-bet levels in FLT3L/TLR8L-primed CD8$^+$ T cells (Fig. 6A, 6B). Moreover, ELA-specific CD8$^+$ T cells primed in the presence of the anti–IL-12p70 blocking Ab expressed considerably less granzyme B and perforin (Fig. 6C) and were also less polyfunctional (Fig. 6D).

Discussion

We report in this study that human PBMCs mobilized with GM-CSF/IL-4 or FLT3L respond differently to maturation signals such as cytokines or TLR ligands, affecting the subsequent quality of the primed CD8$^+$ T cell response. Combined use of FLT3L and TLR8L resulted in the priming of Ag-specific CD8$^+$ T cells displaying robust effector functions, thereby showing that a selective TLR8 agonist can act as a potent adjuvant to prime functionally superior Ag-specific human CD8$^+$ T cells. Collectively, our data indicate that TLR8L, through effects on FLT3L-mobilized DCs, triggers T-bet expression

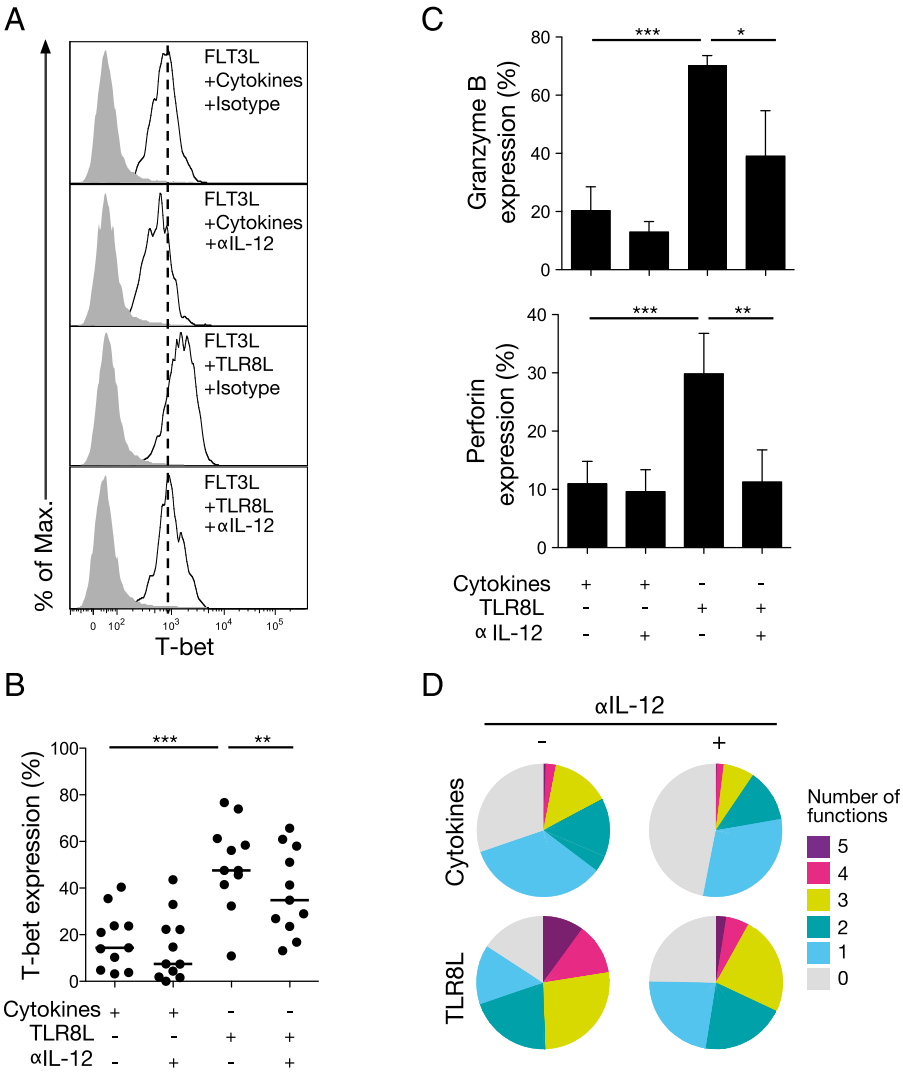

FIGURE 6. IL-12–dependent functional quality of FLT3L/TLR8L-primed CD8$^+$ T cells. (**A**) Representative flow cytometry plots showing intracellular T-bet expression (white histograms) by ELA-specific CD8$^+$ T cells primed with FLT3L plus the indicated maturation signals in the presence of an anti–IL-12p70 blocking Ab or a mouse IgG1 isotype control Ab. Gray histograms depict isotype control staining and vertical dotted lines indicate the mean fluorescence intensity (MFI) of T-bet staining for the weakest priming condition. (**B**) Intracellular T-bet expression by ELA-specific CD8$^+$ T cells primed under different conditions. Horizontal bars indicate median values. (**C**) Granzyme B (*top graph*) and perforin (*bottom graph*) expression by ELA-specific CD8$^+$ T cells primed as in (B). Data are averaged over eight independent experiments. Error bars indicate SD from the mean. Statistical comparisons between groups were performed using the Wilcoxon signed rank test: $*p < 0.05$, $**p < 0.01$, $***p < 0.001$. (**D**) Polyfunctional profiles of ELA-specific CD8$^+$ T cells primed as in (B). Data are averaged over two independent experiments with ELA peptide–pulsed HLA-A2$^+$ B-LCL target cells.

in primed CD8$^+$ T cells via an IL-12–dependent mechanism. In turn, T-bet endows these CD8$^+$ T cells with superior Ag sensitivity, robust cytolytic activity, and polyfunctionality. We also demonstrate that the enhanced Ag sensitivity of FLT3L/TLR8L-primed CD8$^+$ T cells does not arise through the selection of T cells bearing high-affinity TCRs during the priming process. Instead, this gain in Ag sensitivity may be explained by a reduction in TCR/pMHCI activation thresholds experienced by FLT3L/TLR8L-primed cells, leaving them poised for Ag-driven activation.

These findings were made possible by the development of an original in vitro priming model that offers several practical and theoretical advantages over existing systems. In addition to streamlining the search for more effective adjuvants, our approach is applicable to several notable challenges in the field. The use of unmanipulated PBMCs in particular will likely aid in the identification of immunization regimens suitable for individuals who are typically refractory to priming with standard vaccines, such as those at the extremes of age or with advanced HIV infection. Moreover, our priming model can be used to study the mechanisms underlying effective T cell priming (e.g., to identify the DC subsets or molecular pathways involved). For instance, preliminary data generated using our approach imply that DCs from the myeloid lineage are most likely to be involved in FLT3L/TLR8L-mediated T cell priming. In contrast to the GM-CSF receptor (CD116), FLT3 (CD135) was not expressed on CD14$^+$ monocytes but was instead localized to plasmacytoid and myeloid DCs (pDCs and mDCs, respectively; data not shown), implicating these subsets in the FLT3L-mediated priming process. Furthermore, experiments involving the magnetic depletion of various microbead-bound APC subsets showed that CD14$^+$ monocytes and pDCs do not affect ELA-specific CD8$^+$ T cell priming with the FLT3L/TLR8L combination. In contrast, the depletion of mDCs had a negative impact on priming in some experiments (data not shown). Thus, mDCs likely play a role in CD8$^+$ T cell priming in the presence of FLT3L and TLR8L, consistent with the fact that TLR8 is expressed by mDCs but not pDCs. However, it is probable that other DC subsets hold the potential to prime CD8$^+$ T cells under these conditions. For instance, FLT3L was recently reported to mobilize a rare population of circulating mDC precursors (39). Finally, our model could facilitate the selection of Ag formulations best suited to the induction of highly functional de novo T cell responses. The use of synthetic long peptides, which display several beneficial features for CD8$^+$ T cell priming compared with short peptides (34, 35, 40, 41), serves as one such example.

We envisage that the in vitro priming approach presented in this study may be useful for screening candidate Ags and adjuvants for vaccination in humans. For instance, the present data encourage further testing of the adjuvant potential and inflammatory properties of selective TLR8 agonists in vivo. Recent work in transgenic mice expressing different levels of human TLR8 supports a role for this receptor in autoimmune inflammation, suggesting that TLR8L use may cause adverse effects in humans (42). However, inflammatory side effects might feasibly be averted through the specific targeting of such an adjuvant directly to lymph nodes, using delivery agents such as amphiphiles (i.e., linking the Ag and adjuvant to a lipophilic albumin-binding tail) or nanoparticles (43, 44). These approaches could be called upon to decrease the systemic dissemination and potential toxicity of TLR8L while boosting CD8$^+$ T cell priming efficacy. In light of our findings, investigating the adjuvant potential of other TLR8 (e.g., ssPoly(U) or the benzoazepine analog TL8-506) or TLR7/8 (e.g., imidazoquinoline R848 or thiazoquinolone CL075) ligands will likely be important. Differences in potency or unexpected antagonistic effects (e.g., between TLR7 and TLR8 signaling pathways) may be observed. Our in vitro priming system may also expedite the generation of potent T cells for adoptive cell therapy. It is notable in this respect that FLT3L/TLR8L-primed Ag-specific CD8$^+$ T cells recognized naturally presented Ags on a tumor cell line and exhibited properties associated with in vivo efficacy. The present findings are therefore directly relevant to our understanding of effector T cell generation and the development of effective immunotherapy in humans.

Acknowledgments

We thank Pedro Romero for providing melanoma cell lines and Robert Seder for constructive discussions.

Disclosures

A.L., R.M., and V.A. are inventors of patent number EP14305080 entitled "Methods for testing T cell priming efficacy in a subject" filed on January 21, 2014. The other authors have no financial conflicts of interest.

References

1. Appay, V., D. C. Douek, and D. A. Price. 2008. CD8$^+$ T cell efficacy in vaccination and disease. *Nat. Med.* 14: 623–628.
2. Seder, R. A., P. A. Darrah, and M. Roederer. 2008. T-cell quality in memory and protection: implications for vaccine design. *Nat. Rev. Immunol.* 8: 247–258.
3. Braumüller, H., T. Wieder, E. Brenner, S. Aßmann, M. Hahn, M. Alkhaled, K. Schilbach, F. Essmann, M. Kneilling, C. Griessinger, et al. 2013. T-helper-1-cell cytokines drive cancer into senescence. *Nature* 494: 361–365.
4. Dutoit, V., V. Rubio-Godoy, P. Y. Dietrich, A. L. Quiqueres, V. Schnuriger, D. Rimoldi, D. Liénard, D. Speiser, P. Guillaume, P. Batard, et al. 2001. Heterogeneous T-cell response to MAGE-A10(254-262): high avidity-specific cytolytic T lymphocytes show superior antitumor activity. *Cancer Res.* 61: 5850–5856.
5. Rosenberg, S. A., J. C. Yang, and N. P. Restifo. 2004. Cancer immunotherapy: moving beyond current vaccines. *Nat. Med.* 10: 909–915.
6. Pulendran, B., and R. Ahmed. 2011. Immunological mechanisms of vaccination. *Nat. Immunol.* 12: 509–517.
7. Banchereau, J., and A. K. Palucka. 2005. Dendritic cells as therapeutic vaccines against cancer. *Nat. Rev. Immunol.* 5: 296–306.
8. Kawai, T., and S. Akira. 2010. The role of pattern-recognition receptors in innate immunity: update on Toll-like receptors. *Nat. Immunol.* 11: 373–384.
9. Coffman, R. L., A. Sher, and R. A. Seder. 2010. Vaccine adjuvants: putting innate immunity to work. *Immunity* 33: 492–503.
10. Jurk, M., F. Heil, J. Vollmer, C. Schetter, A. M. Krieg, H. Wagner, G. Lipford, and S. Bauer. 2002. Human TLR7 or TLR8 independently confer responsiveness to the antiviral compound R-848. *Nat. Immunol.* 3: 499.
11. Gorden, K. B., K. S. Gorski, S. J. Gibson, R. M. Kedl, W. C. Kieper, X. Qiu, M. A. Tomai, S. S. Alkan, and J. P. Vasilakos. 2005. Synthetic TLR agonists reveal functional differences between human TLR7 and TLR8. *J. Immunol.* 174: 1259–1268.
12. Steinhagen, F., T. Kinjo, C. Bode, and D. M. Klinman. 2011. TLR-based immune adjuvants. *Vaccine* 29: 3341–3355.
13. Sallusto, F., and A. Lanzavecchia. 1994. Efficient presentation of soluble antigen by cultured human dendritic cells is maintained by granulocyte/macrophage colony-stimulating factor plus interleukin 4 and downregulated by tumor necrosis factor α. *J. Exp. Med.* 179: 1109–1118.
14. Wölfl, M., and P. D. Greenberg. 2014. Antigen-specific activation and cytokine-facilitated expansion of naive, human CD8$^+$ T cells. *Nat. Protoc.* 9: 950–966.
15. Martinuzzi, E., G. Afonso, M. C. Gagnerault, G. Naselli, D. Mittag, B. Combadière, C. Boitard, N. Chaput, L. Zitvogel, L. C. Harrison, and R. Mallone. 2011. acDCs enhance human antigen-specific T-cell responses. *Blood* 118: 2128–2137.
16. Altman, J. D., P. A. H. Moss, P. J. R. Goulder, D. H. Barouch, M. G. McHeyzer-Williams, J. I. Bell, A. J. McMichael, and M. M. Davis. 1996. Phenotypic analysis of antigen-specific T lymphocytes [published erratum appears in Science 1998 Jun 19;280(5371):1821]. *Science* 274: 94–96.
17. Price, D. A., J. M. Brenchley, L. E. Ruff, M. R. Betts, B. J. Hill, M. Roederer, R. A. Koup, S. A. Migueles, E. Gostick, L. Wooldridge, et al. 2005. Avidity for antigen shapes clonal dominance in CD8$^+$ T cell populations specific for persistent DNA viruses. *J. Exp. Med.* 202: 1349–1361.
18. Purbhoo, M. A., J. M. Boulter, D. A. Price, A. L. Vuidepot, C. S. Hourigan, P. R. Dunbar, K. Olson, S. J. Dawson, R. E. Phillips, B. K. Jakobsen, et al. 2001. The human CD8 coreceptor effects cytotoxic T cell activation and antigen sensitivity primarily by mediating complete phosphorylation of the T cell receptor zeta chain. *J. Biol. Chem.* 276: 32786–32792.
19. Whelan, J. A., P. R. Dunbar, D. A. Price, M. A. Purbhoo, F. Lechner, G. S. Ogg, G. Griffiths, R. E. Phillips, V. Cerundolo, and A. K. Sewell. 1999. Specificity of CTL interactions with peptide-MHC class I tetrameric complexes is temperature dependent. *J. Immunol.* 163: 4342–4348.
20. Papagno, L., J. R. Almeida, E. Nemes, B. Autran, and V. Appay. 2007. Cell permeabilization for the assessment of T lymphocyte polyfunctional capacity. *J. Immunol. Methods* 328: 182–188.

21. Almeida, J. R., D. Sauce, D. A. Price, L. Papagno, S. Y. Shin, A. Moris, M. Larsen, G. Pancino, D. C. Douek, B. Autran, et al. 2009. Antigen sensitivity is a major determinant of CD8$^+$ T-cell polyfunctionality and HIV-suppressive activity. *Blood* 113: 6351–6360.
22. Larsen, M., D. Sauce, L. Arnaud, S. Fastenackels, V. Appay, and G. Gorochov. 2012. Evaluating cellular polyfunctionality with a novel polyfunctionality index. *PLoS One* 7: e42403.
23. Martinuzzi, E., M. Scotto, E. Enée, V. Brezar, J. A. Ribeil, P. van Endert, and R. Mallone. 2008. Serum-free culture medium and IL-7 costimulation increase the sensitivity of ELISpot detection. *J. Immunol. Methods* 333: 61–70.
24. Guermonprez, P., J. Helft, C. Claser, S. Deroubaix, H. Karanje, A. Gazumyan, G. Darasse-Jèze, S. B. Telerman, G. Breton, H. A. Schreiber, et al. 2013. Inflammatory Flt3l is essential to mobilize dendritic cells and for T cell responses during *Plasmodium* infection. *Nat. Med.* 19: 730–738.
25. Pulendran, B., J. Banchereau, S. Burkeholder, E. Kraus, E. Guinet, C. Chalouni, D. Caron, C. Maliszewski, J. Davoust, J. Fay, and K. Palucka. 2000. Flt3-ligand and granulocyte colony-stimulating factor mobilize distinct human dendritic cell subsets in vivo. *J. Immunol.* 165: 566–572.
26. Parajuli, P., R. L. Mosley, V. Pisarev, J. Chavez, A. Ulrich, M. Varney, R. K. Singh, and J. E. Talmadge. 2001. Flt3 ligand and granulocyte-macrophage colony-stimulating factor preferentially expand and stimulate different dendritic and T-cell subsets. *Exp. Hematol.* 29: 1185–1193.
27. Xu, Y., Y. Zhan, A. M. Lew, S. H. Naik, and M. H. Kershaw. 2007. Differential development of murine dendritic cells by GM-CSF versus Flt3 ligand has implications for inflammation and trafficking. *J. Immunol.* 179: 7577–7584.
28. Pittet, M. J., D. Valmori, P. R. Dunbar, D. E. Speiser, D. Liénard, F. Lejeune, K. Fleischhauer, V. Cerundolo, J. C. Cerottini, and P. Romero. 1999. High frequencies of naive Melan-A/MART-1-specific CD8$^+$ T cells in a large proportion of human histocompatibility leukocyte antigen (HLA)-A2 individuals. *J. Exp. Med.* 190: 705–715.
29. Dutoit, V., V. Rubio-Godoy, M. J. Pittet, A. Zippelius, P. Y. Dietrich, F. A. Legal, P. Guillaume, P. Romero, J. C. Cerottini, R. A. Houghten, et al. 2002. Degeneracy of antigen recognition as the molecular basis for the high frequency of naive A2/Melan-a peptide multimer$^+$CD8$^+$ T cells in humans. *J. Exp. Med.* 196: 207–216.
30. Pinto, S., D. Sommermeyer, C. Michel, S. Wilde, D. Schendel, W. Uckert, T. Blankenstein, and B. Kyewski. 2014. Misinitiation of intrathymic MART-1 transcription and biased TCR usage explain the high frequency of MART-1-specific T cells. *Eur. J. Immunol.* 44: 2811–2821.
31. Romero, P., D. E. Speiser, and N. Rufer. 2014. Deciphering the unusual HLA-A2/Melan-A/MART-1-specific TCR repertoire in humans. *Eur. J. Immunol.* 44: 2567–2570.
32. Romero, P., D. Valmori, M. J. Pittet, A. Zippelius, D. Rimoldi, F. Lévy, V. Dutoit, M. Ayyoub, V. Rubio-Godoy, O. Michielin, et al. 2002. Antigenicity and immunogenicity of Melan-A/MART-1 derived peptides as targets for tumor reactive CTL in human melanoma. *Immunol. Rev.* 188: 81–96.
33. Joffre, O. P., E. Segura, A. Savina, and S. Amigorena. 2012. Cross-presentation by dendritic cells. *Nat. Rev. Immunol.* 12: 557–569.
34. Chauvin, J. M., P. Larrieu, G. Sarrabayrouse, A. Prévost-Blondel, R. Lengagne, J. Desfrançois, N. Labarrière, and F. Jotereau. 2012. HLA anchor optimization of the melan-A-HLA-A2 epitope within a long peptide is required for efficient cross-priming of human tumor-reactive T cells. *J. Immunol.* 188: 2102–2110.
35. Rosalia, R. A., E. D. Quakkelaar, A. Redeker, S. Khan, M. Camps, J. W. Drijfhout, A. L. Silva, W. Jiskoot, T. van Hall, P. A. van Veelen, et al. 2013. Dendritic cells process synthetic long peptides better than whole protein, improving antigen presentation and T-cell activation. *Eur. J. Immunol.* 43: 2554–2565.
36. Iglesias, M. C., J. R. Almeida, S. Fastenackels, D. J. van Bockel, M. Hashimoto, V. Venturi, E. Gostick, A. Urrutia, L. Wooldridge, M. Clement, et al. 2011. Escape from highly effective public CD8$^+$ T-cell clonotypes by HIV. *Blood* 118: 2138–2149.
37. Glimcher, L. H., M. J. Townsend, B. M. Sullivan, and G. M. Lord. 2004. Recent developments in the transcriptional regulation of cytolytic effector cells. *Nat. Rev. Immunol.* 4: 900–911.
38. Takemoto, N., A. M. Intlekofer, J. T. Northrup, E. J. Wherry, and S. L. Reiner. 2006. Cutting edge: IL-12 inversely regulates T-bet and eomesodermin expression during pathogen-induced CD8$^+$ T cell differentiation. *J. Immunol.* 177: 7515–7519.
39. Breton, G., J. Lee, Y. J. Zhou, J. J. Schreiber, T. Keler, S. Puhr, N. Anandasabapathy, S. Schlesinger, M. Caskey, K. Liu, and M. C. Nussenzweig. 2015. Circulating precursors of human CD1c$^+$ and CD141$^+$ dendritic cells. *J. Exp. Med.* 212: 401–413.
40. Bijker, M. S., S. J. van den Eeden, K. L. Franken, C. J. Melief, R. Offringa, and S. H. van der Burg. 2007. CD8$^+$ CTL priming by exact peptide epitopes in incomplete Freund's adjuvant induces a vanishing CTL response, whereas long peptides induce sustained CTL reactivity. *J. Immunol.* 179: 5033–5040.
41. Melief, C. J., and S. H. van der Burg. 2008. Immunotherapy of established (pre) malignant disease by synthetic long peptide vaccines. *Nat. Rev. Cancer* 8: 351–360.
42. Guiducci, C., M. Gong, A. M. Cepika, Z. Xu, C. Tripodo, L. Bennett, C. Crain, P. Quartier, J. J. Cush, V. Pascual, et al. 2013. RNA recognition by human TLR8 can lead to autoimmune inflammation. *J. Exp. Med.* 210: 2903–2919.
43. Liu, H., K. D. Moynihan, Y. Zheng, G. L. Szeto, A. V. Li, B. Huang, D. S. Van Egeren, C. Park, and D. J. Irvine. 2014. Structure-based programming of lymph-node targeting in molecular vaccines. *Nature* 507: 519–522.
44. Jeanbart, L., M. Ballester, A. de Titta, P. Corthésy, P. Romero, J. A. Hubbell, and M. A. Swartz. 2014. Enhancing efficacy of anticancer vaccines by targeted delivery to tumor-draining lymph nodes. *Cancer Immunol. Res.* 2: 436–447.